Conversion of p35 to p25 deregulates Cdk5 activity and promotes neurodegeneration

Gentry N. Patrick*, Lawrence Zukerberg*†, Margareta Nikolic*‡, Suzanne de la Monte†§, Pieter Dikkes‖ & Li-Huei Tsai*¶

* *Department of Pathology, Harvard Medical School and* ¶*Howard Hughes Medical Institute, 200 Longwood Avenue, Boston, Massachusetts 02115, USA*
† *Department of Pathology, Massachusetts General Hospital, Boston, Massachusetts 02114, USA*
§ *Massachusetts General Hospital—East Cancer Center, Charlestown, Massachusetts 02119, USA*
‖ *Department of Neurology, Children's Hospital, 300 Longwood Avenue, Boston, Massachusetts 02115, USA*
‡ *Present address: Molecular Neurobiology Group, King's College London, London SE1 9RT, UK*

Cyclin-dependent kinase 5 (Cdk5) is required for proper development of the mammalian central nervous system. To be activated, Cdk5 has to associate with its regulatory subunit, p35. We have found that p25, a truncated form of p35, accumulates in neurons in the brains of patients with Alzheimer's disease. This accumulation correlates with an increase in Cdk5 kinase activity. Unlike p35, p25 is not readily degraded, and binding of p25 to Cdk5 constitutively activates Cdk5, changes its cellular location and alters its substrate specificity. *In vivo* the p25/Cdk5 complex hyperphosphorylates tau, which reduces tau's ability to associate with microtubules. Moreover, expression of the p25/Cdk5 complex in cultured primary neurons induces cytoskeletal disruption, morphological degeneration and apoptosis. These findings indicate that cleavage of p35, followed by accumulation of p25, may be involved in the pathogenesis of cytoskeletal abnormalities and neuronal death in neurodegenerative diseases.

Cdk5 is a small protein serine/threonine kinase with close structural homology to the mitotic CDKs[1,2]. Association of Cdk5 with p35, its regulatory subunit, is critical for kinase activation[3–5]. The p35/Cdk5 kinase is required for neurite growth, as inactivation of Cdk5 in cultured cortical or cerebellar neurons inhibits neurite outgrowth[6,7]. Mice lacking p35 display defects in cortical lamination and fasciculation of axon fibres[8–10]. Interestingly, in $p35^{-/-}$ cortex, the layering of cortical neurons is inverted, presumably because neurons born later cannot migrate past their predecessors[9]. Cdk5-null mice are not viable past postnatal day 0 (ref. 11). These animals have extensive abnormalities in the CNS including cortical and hippocampal lamination defects and cerebellar hypoplasia[12]. These studies underscore the critical role of the p35/Cdk5 kinase in CNS development. Cdk5 activity is also required in the mature nervous system. Phosphorylation of DARPP32 by Cdk5 makes it an inhibitor of protein kinase A and alters the responses of striatal neurons to dopamine[13]. Cdk5 also phosphorylates Munc18, which in turn affects synaptic vesicle exocytosis[14].

Alzheimer's disease (AD) is a degenerative disease characterized by progressive loss of neurons; its principal clinical manifestation is dementia. The main pathological features of AD include amyloid plaques, which are deposited extracellularly, and cytoplasmic filamentous materials known as neurofibrillary tangles (NFT), which accumulate in the neuronal cell soma. Many studies have led to the conclusion that aberrantly phosphorylated forms of the microtubule-associated protein tau are the main constituents of NFT in the brains of patients with AD[15,16]. Here we show that deregulation of Cdk5 contributes to the pathogenesis of neurodegenerative diseases such as AD. Deregulation of Cdk5 is caused by the accumulation of a truncated fragment of p35, p25, which is produced and accumulates in the brains of patients with AD. p25 causes Cdk5 to be constitutively activated and mislocalized *in vivo*. The p25/Cdk5 kinase phosphorylates tau efficiently and reduces the ability of tau to bind to microtubules. Moreover, p25/Cdk5 causes morphological degeneration and profound apoptotic cell death of primary neurons. These observations indicate that the conversion of p35 to p25 is involved in the pathogenesis of AD.

Table 1 Case details

Age (years)	Sex	Diagnosis	Postmortem delay (h)	Lane
89	N/A	Control	<18	1
66	M	Control	<24	2
45	F	Control	<24	3
72	F	AD	3	4
59	F	AD	<18	5
71	F	AD	<18	6
64	F	AD	4.5	7
73	F	AD	14	8
66	N/A	Control	<18	9
N/A	N/A	HD	<24	10
78	F	AD	<18	11
68	M	AD	<18	12
87	M	AD	<18	13

N/A = not available

p25 accumulates in the brains of AD patients

We surveyed the expression profiles of p35 and Cdk5 from human brain tissues (Table 1). Whereas p35 levels were similar in all samples, a species with a relative molecular mass of 25,000 (M_r=25K), recognizable by anti-p35 antibodies, was found to be accumulated 20–40-fold (arrowhead) compared to p35 in all but one of the samples from patients with AD (Fig. 1a). Cdk5 levels do not vary significantly between normal and AD samples. Table 1 summarizes the cases used in this study. Figure 1a (lane 8) represents a sample from a patient in the terminal stages of AD with a substantial loss of brain tissue (brain weight of 950 g), which may account for the lack of accumulation of the 25K species. To verify the identity of the 25K species, we used antibodies recognizing various regions of p35 (Fig. 1c). p35 is the most prominent protein recognized by these antibodies in rat brain lysate, as detected by western blot analysis (Fig. 1d). The accumulation of this 25K species in samples from AD patients corresponded to the elevated Cdk5 kinase activity in the AD samples, as indicated by the Cdk5-associated histone H1 kinase activity (Fig. 1b). p35 is phosphorylated in a Cdk5 immunoprecipitation/kinase assay; the 25K species was found to be similarly phosphorylated (Fig. 1b). This 25K species was contained in immunocomplexes that were immunoprecipitated

with either anti-Cdk5 antibodies (Fig. 1b) or antibodies recognizing the carboxy-terminal portion of p35 (Fig. 1e, right), indicating that the 25K species is either a cleavage product of p35 or derived from a related protein. Amino-terminal-specific anti-p35 antibodies did not recognize the 25K species (Fig. 1e, left). The size of the 25K species is reminiscent of p25, which was previously copurified with Cdk5 from bovine brain lysates[3–5,17]. Indeed, the 25K species comigrated with p25 from COS-7 cell lysates transfected with cytomegalovirus (CMV)–p25 (a p35 N-terminal deletion mutant generated according to the published sequences) on SDS-polyacrylamide gel electrophoresis (SDS-PAGE) (Fig. 1e, right). To determine whether the 25K species observed in brain lysates from AD patients is actually p25, the V8 digest pattern of the 25K species from AD tissue was compared to that of p25 derived from COS-7 cell lysate transfected with CMV-p25. The two were identical (Fig. 1f). On the basis of the observations that the 25K species is recognized by the p35 C-terminal-specific antibodies but not by the N-terminal-specific antibodies, that it associates with Cdk5 and with Cdk5 kinase activity, that it comigrates with p25 on SDS-PAGE and that it displays an identical V8 digestion pattern to that of recombinant p25, we conclude that the 25K species that accumulates in the brains of AD patients is indeed p25. As p35 is encoded by one exon, without interruption by introns, alternative splicing cannot account for the production of p25; rather, it is probably generated by proteolytic cleavage at a specific site (Fig. 1c).

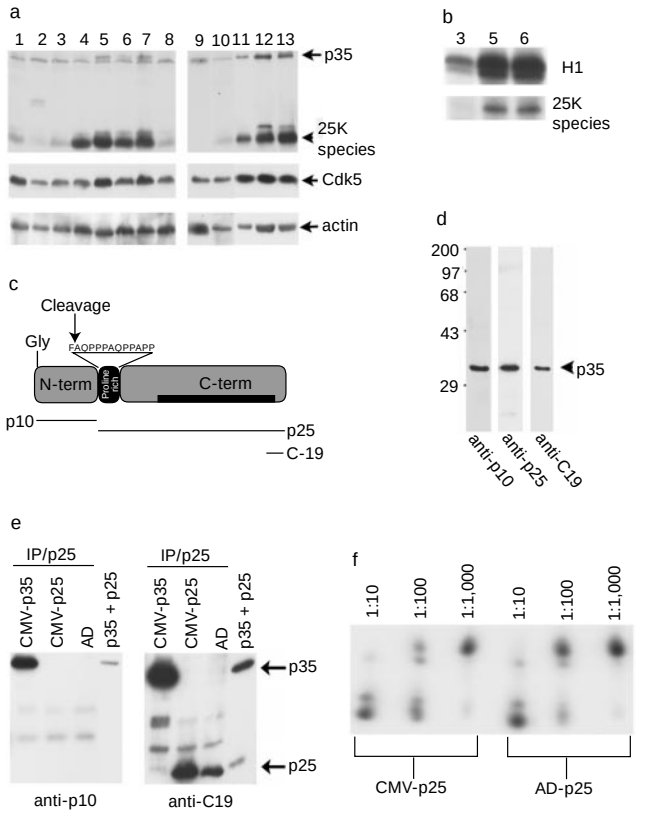

Figure 1 Accumulation of p25 in brain lysates from patients with AD. **a**, p35, Cdk5 and actin western blots of brain lysates from normal control (lanes 1–3 and 9) and AD tissues (lanes 4–8 and 11–13). Lane 10 is from a Huntington's disease patient. **b**, Cdk5 immunoprecipitation (IP)/kinase assays of control (lane 3) and AD (lanes 5 and 6) brain lysates using Cdk5 antibodies. Histone H1 was used as exogenous substrate. The 25K species was also immunoprecipitated and phosphorylated in the Cdk5 IP/kinase assay. **c**, Structure of p35. The N- and C-terminal regions of p35 are separated by a proline-rich region (black box); the minimal Cdk5 binding and activation domain is marked by thin black bar within the C-terminal region; cleavage between the phenylalanine and alanine residues liberates a 25K species. C-19 and p25 polyclonal antibodies recognize p35 and p25. p10 polyclonal antibodies recognize p35 only. **d**, Western blot analysis of P0 rat brain lysate probed with p10, C-19 and p25-specific antibodies. Left, M_r ($\times 10^3$). **e**, p25 antibody immunoprecipitates of lysates from COS-7 cells transfected with CMV–p35 or CMV–p25 and AD brain, and western blot with either p10 N-terminal-specific or C-19 C-terminal-specific antibodies; p35 + p25 represents a mixture of CMV–p35- and CMV–p25-transfected lysates. **f**, V8 protease-digested fingerprints comparing recombinant p25 to the 25K species (previously immunoprecipitated and phosphorylated in Cdk5 IP/kinase reactions) identified in AD brain lysates.

p25 is found in neurons containing NFT in AD brain

As the levels of p25 protein were elevated in brain lysates from AD patients, it was of interest to determine the distribution of p25 immunoreactivity in histological sections from AD and control brain. The p25 polyclonal antibody labelled certain neurons in sections taken from the hippocampal formation of patients with AD (Fig. 2b). This antibody otherwise labelled the periphery of the perikaryon of hippocampal neurons in both AD and control sections (Fig. 2a). Adjacent sections were stained with AT8 (ref. 18), an anti-phospho-tau antibody, which labelled neurons containing NFT in the brains of AD patients (Fig. 2d) but not in control

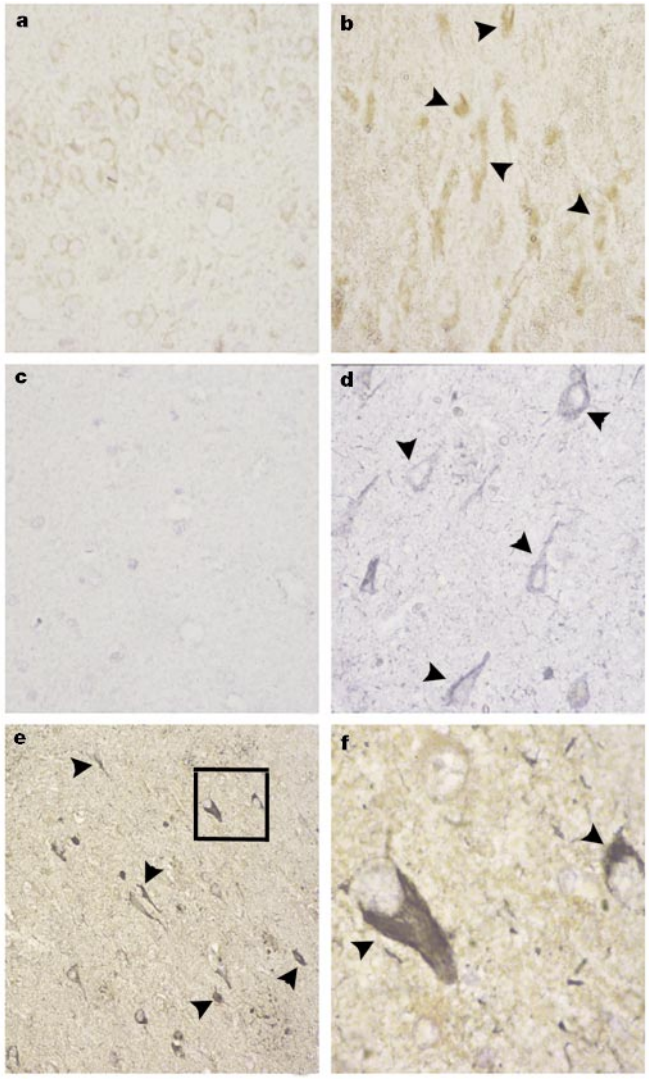

Figure 2 Immunohistochemistry of normal control and AD hippocampal sections. **a**, Control labelled with p25 antibody. **b**, AD labelled with p25 antibody (brown, arrowheads). **c**, Control labelled with AT8 (blue-grey). **d**, AD labelled with AT8 (blue-grey, arrowheads). **e**, AD labelled with p25 antibody (brown) and AT8 (blue-grey) detecting neurons containing NFT; double labelling appears blue-black (arrowheads). **f**, Inset from **e**; neurons double-labelled with p25 and AT8 antibodies (arrowheads). Original magnifications are 200× for **a–d**, 100× for **e** and 500× for **f**.

sections (Fig. 2c). Double immunostaining with anti-p25 and AT8 revealed that many NFT-containing neurons were also positive for p25 (Fig. 2e, f). However, there were more neurons with elevated p25 immunoreactivity than neurons displaying NFT (Fig. 2b, d). We also carried out immunostaining with anti-p10 antibodies, which detect only full-length p35 (Fig. 1c). Anti-p10 also labelled the neuronal periphery in control sections; its immunoreactivity did not accumulate in neurons containing NFT (data not shown). Together, western blot analysis and immunohistochemistry of AD tissues indicate that p25, but not p35, may accumulate in the brains of patients with AD and be present in neurons affected by neurodegeneration.

p25 differs from p35 in distribution and stability

p25 contains all the elements required for Cdk5 activation (Fig. 1c) and activates Cdk5 *in vitro*[3,19]. As p25, but not p35, accumulates in AD, we attempted to determine whether these two proteins have different biochemical properties. Both Cdk5 and p35 are enriched in the processes and growth cones of neurons and p35 segregates with the plasma membrane[6,20]. Figure 3a shows an N-terminal myristoylation signal motif that is highly conserved in mammalian, *Xenopus*[21] and *Caenorhabditis elegans* p35 homologues. To determine whether this myristoylation signal is required for the normal subcellular localization of p35, the conserved glycine at position 2 (Fig. 3a) was mutated to alanine and expressed in COS-7 cells (Fig. 3b). Although p35 was localized at the cell periphery and induced lamellipodia and filopodia (Fig. 3b, left; and ref. 20), the G2A mutant was absent at the cell periphery (Fig. 3b, right), showing that the myristoylation signal is essential for the proper distribution of p35. As p25 lacks the conserved myristoylation sequence we compared its subcellular localization with that of p35 in transfected fibroblasts. Figure 3c shows that p25 was enriched in nuclear and perinuclear regions of the cell, whereas p35 and p10 (an N-terminal fragment of p35 lacking the p25 region) were localized and enriched, in the case of p10, at the cell peripheries. We further investigated the distribution of p25 by subcellular fractionation. Figure 3d shows that, although p35 was more abundant in the membrane fraction, p25 was enriched in the cytosolic fraction. This may indicate that p35 is normally targeted to the membrane *in vivo*. In contrast, p25, which is not targeted to the plasma membrane, probably sequesters Cdk5 away from compartments of the cell where p35/Cdk5 activity is normally required. In addition, in primary cortical neurons, p25 is primarily concentrated in the cell soma and is largely absent from neurites (see below), whereas p35 is present in the peripheries and nerve terminals[6,20].

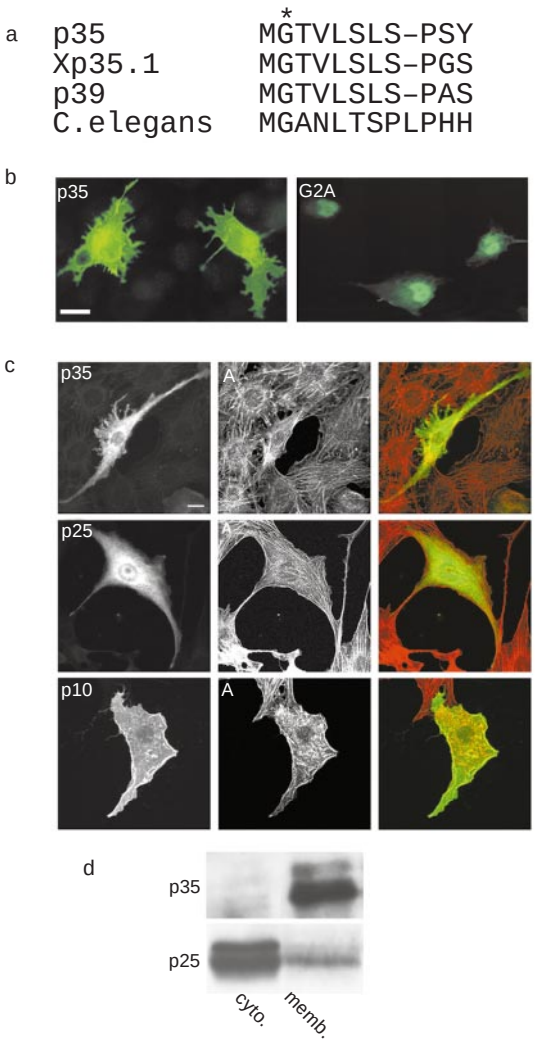

Figure 3 p35 but not p25 is associated with peripheral membranes. **a**, Myristoylation sequence within p35 homologues is conserved. **b**, COS-7 cells were transfected with either wild-type p35 or the p35 G2A mutant followed by p35 immunostaining. **c**, Confocal immunofluoresence of Swiss 3T3 cells transfected with p35, p25 or p10–HA (overlay: red, rhodamine-conjugated phalloidin, labelled A for actin; green, p35, p25 or p10–HA). All scale bars are 10 μm. **d**, Subcellular distribution of p35 and p25 in fractionated COS-7 cell lysates after transfection.

In addition to the difference in subcellular localization of p35 and p25, there is a marked difference in turnover rate between the two. Our previous studies indicated that Cdk5 activity is tightly regulated by p35 protein levels[22]. p35 has a half-life ($t_{1/2}$) of ~20–30 min in primary cortical neurons; this rapid turnover rate is in part due to phosphorylation-stimulated, ubiquitin-mediated degradation[22]. When expressed in COS-7 cells together with Cdk5, p25 had a ~5–10-fold longer half-life than p35 or the p35 G2A mutant (Fig. 4a, b). Cdk5-associated histone H1 kinase activity paralleled the levels of p35 or p25. These observations indicate that the accumulated p25 in the brains of AD patients may cause prolonged activation of Cdk5 and mislocalization of Cdk5 kinase activity in affected neurons.

Tau phosphorylation by the p25/Cdk5 kinase *in vivo*

To explore further the functional difference between the p35/Cdk5 and p25/Cdk5 kinases *in vivo*, we compared the activity of these two

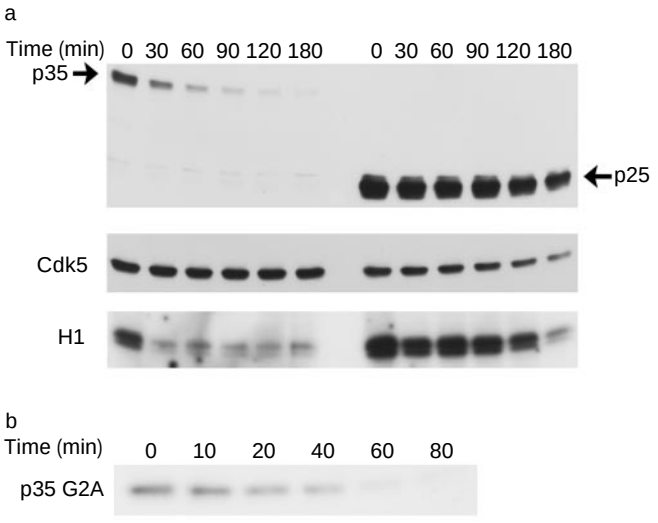

Figure 4 p25 is a stable protein. Western blots of lysates from cycloheximide treatment half-life experiments of p35 and p25 (**a**) and the p35 G2A mutant (**b**) in transfected COS-7 cells. Also in **a**, western blot analysis of Cdk5 and *in vitro* Cdk5-associated histone H1 kinase assays from lysates used in cycloheximide treatment half-life experiments.

kinases in phosphorylation of the microtubule-associated protein tau. Tau is a substrate of Cdk5 (ref. 23). A His_6-tagged human tau 40 (his_6–htau40) was cotransfected with p35/Cdk5, p25/Cdk5 or p25/DNK5 (a catalytically inactive mutant of Cdk5) in COS-7 cells. Tau phosphorylation was evaluated by immunoblotting with AT8 or PHF-1. AT8 recognizes tau epitopes phosphorylated at Ser 202 and Ser 205 and PHF-1 recognizes epitopes phosphorylated at and around Thr 396, sites previously shown to be phosphorylated by Cdk5 *in vitro*[24–27]. Intense AT8 immunoreactivity was seen in cells expressing p25/Cdk5 (Fig. 5a, lane 5) but not p35/Cdk5 or p25/DNK5 (Fig. 5a, lanes 3 and 6). Interestingly, PHF-1 detected a slower migrating species in the p25/Cdk5 expressing cells (Fig. 5a, lane 5 and 5b, arrowhead) which was readily abolished upon protein phosphatase treatment (Fig. 5a, lanes 8 and 9), indicating that this slower migrating band was indeed a phosphorylated species of tau. This species was not present in cells expressing p35/Cdk5 or p25/DNK5. As a control, Fig. 5a (lane 7) shows that GSK3-β, a well established kinase for tau[28,29], caused a large increase in tau PHF-1 immunoreactivity.

Owing to the difference in turnover rate, the steady-state levels of p35 were always much lower than those of p25 (Fig. 5a), which may have contributed to the observed difference in tau phosphorylation. To compare the ability of these kinases to phosphorylate tau when similar levels of the two kinases are expressed *in vivo*, we used five times more p35 than p25 plasmid DNA for transfection. However, even after p35 and p25 were expressed at comparable levels, the slower migrating PHF-1 immunoreactive species of tau was still absent from p35/Cdk5 transfected cells. This is despite the observed increase in PHF-1 immunoreactivity (Fig. 5b), indicating that other differences such as the altered subcellular distribution of the p25/Cdk5 kinase may allow more efficient targeting of tau *in vivo*. Comparable levels of tau were expressed, as indicated by immunoblotting with anti-His_6 antibodies (Fig. 5a). Anti-His_6 antibodies also revealed a shift in tau mobility in cells cotransfected with p25 and Cdk5 (Fig. 5a, lane 5). Transfection of p25 alone did not cause a noticeable increase in PHF-1 or AT8 immunoreactivity, which is likely to reflect the low endogenous level of Cdk5 in COS-7 cells (Fig. 5a, lane 4). When transfected COS-7 cell lysates were incubated with polymerized microtubules, tau's ability to bind microtubules was impaired in cells co-expressing the active p25/Cdk5 kinase complex (Fig. 5c), indicating that the hyperphosphorylation of tau by p25/Cdk5 may affect its function *in vivo*.

p25/Cdk5 causes cytoskeletal disruption

The effects of p25/Cdk5 on tau hyperphosphorylation were also investigated in primary cortical neurons using a herpes simplex recombinant viral expression system. After infection with a βgal virus, weak PHF-1 immunoreactivity was present in the cell soma and axon fibres (Fig. 6a, d). In contrast, infection with p25/Cdk5 produced robust PHF-1 immunoreactivity which was concentrated in the cell soma (Fig. 6b, e, h, i). This effect was reversed when p25/DNK5 was expressed (Fig. 6c, f), indicating that the catalytic activity of Cdk5 is necessary for the observed increase in PHF-1 signal. Neurons infected with p35/Cdk5 also displayed increased PHF-1 immunoreactivity, but to a lesser extent (Fig. 6g). Similar results were obtained using AT8 antibodies (Fig. 6j–k). Many p25/Cdk5-infected neurons, indicated by PHF-1-positive staining, exhibited neurite retraction (Figs 6h, i, 7b–c and f–g), whereas cultures infected with p35/Cdk5 seldom exhibited signs of neurite degeneration (Fig. 6g). Neurofilaments are also well established substrates of Cdk5 (refs 1, 3, 30–32). Using SMI34, a phospho-specific neurofilament H antibody, we observed intense phospho-neurofilament immunoreactivity in p25/Cdk5-infected neurons (Fig. 6m, n, arrowheads), but less intense staining in uninfected neurons (arrows), indicating that the p25/Cdk5 kinase may cause hyperphosphorylation of neurofilaments.

Tau hyperphosphorylation causes microtubule destabilization[16,33]. We have shown that p25/Cdk5-phosphorylated tau binds to microtubules less well. We therefore used a silver-based stain to assess the cytoskeletal integrity of p25/Cdk5-expressing neurons. Figure 6o shows that silver-positive neurons were frequently seen in the p25/Cdk5-expressing cultures (arrows). Silver labelling was specific to p25/Cdk5-infected neurons and was never observed in cultures infected with βgal, p35/Cdk5 or p25/DNK5 (data not shown). These data indicate that p25/Cdk5 may be more potent than p35/Cdk5 in phosphorylating protein substrates such as tau and neurofilaments *in vivo*, which may be, in part, attributable to its accumulation and different localization. Furthermore, they indicate that the presence and accumulation of the p25/Cdk5 kinase is associated with morphological degeneration and cytoskeletal disruption in neurons, events seen in AD and other neurodegenerative diseases.

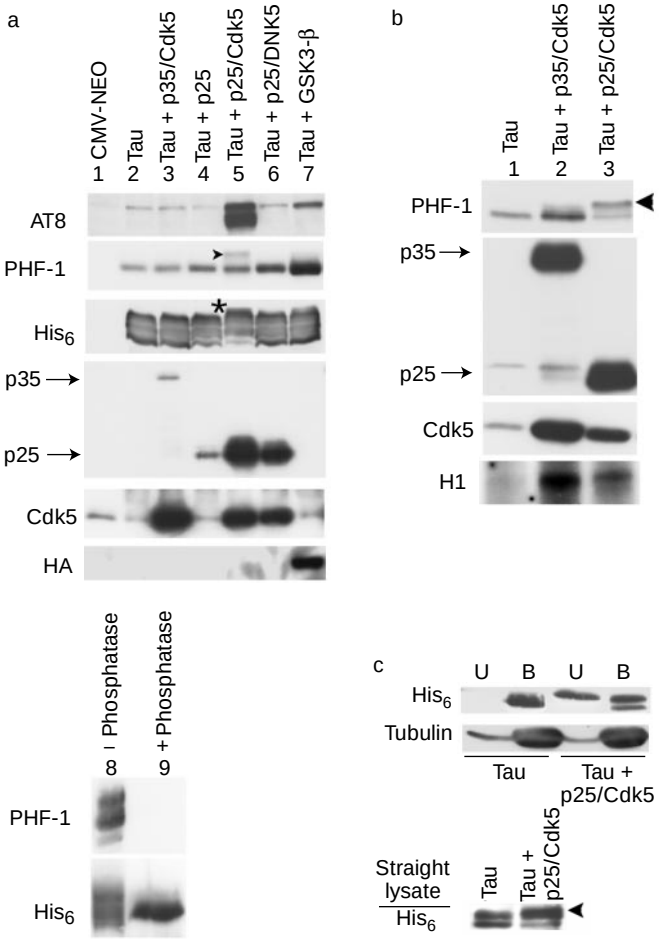

Figure 5 Comparison of tau phosphorylation by p35/Cdk5 and p25/Cdk5. **a**, COS-7 cell lysates transfected with empty vector (lane 1), his_6–htau40 alone (lane 2) or with p35/Cdk5 (lane 3), p25 (lane 4), p25/Cdk5 (lane 5, 8, and 9), p25/DNK5 (lane 6) or HA-tagged GSK3-β (lane 7) CMV expression constructs and probed with phospho-specific tau antibodies AT8 and PHF-1, and anti-His_6, p35, Cdk5 and 12CA5 (HA) antibodies. Arrowhead and asterisk indicate slower migrating phospho-species of tau. Lanes 8 and 9, immunoprecipitation of lysate from lane 5 with anti-His_6 and probed with PHF-1 and anti-His_6 after treatment with buffer alone (lane 8) or potato acid phosphatase (lane 9). **b**, As in **a**, except comparable levels of p35 and p25 were expressed in COS-7 cells after using 5-fold more p35 plasmid DNA; arrowhead indicates shift in tau phosphorylation by p25/Cdk5, absent in p35/Cdk5-transfected cells. **c**, Microtubule-binding assay of COS-7 cells transfected with tau and tau plus p25/Cdk5. U, tau unbound to microtubules; B, tau bound to microtubules. Whereas tau from cells transfected with tau alone all bound to microtubules, a large portion of tau from cells transfected with tau plus p25/Cdk5 was present in the unbound fraction (arrowhead denotes slower migrating species of tau).

The p25/Cdk5 kinase induces apoptosis in neurons

To characterize the cytoskeletal abnormalities further we stained for β-tubulin in the infected cultures. β-tubulin staining revealed a marked difference in the microtubule networks of p25/Cdk5-infected cells compared with those of p25/DNK5- or control βgal-infected cells (Fig. 7a–h). Tubulin was normally distributed throughout the cell soma and the axonal and dendritic compartments in βgal- and p25/DNK5-infected cultures (Fig. 7a, e and d, h, respectively). In contrast, tubulin was concentrated in the perikarya of p25/Cdk5-infected cells (Fig. 7f, g, arrowheads). In fact, most of the p25/Cdk5-infected cells were devoid of neurites. Apoptotic cell bodies were frequently observed in p25/Cdk5-infected cultures (Fig. 7f, arrows), but not in cultures infected with βgal or p25/DNK5 (Fig. 7e, h).

We also found in COS-7 cell transfection experiments that many cells died upon co-expression of p25 and Cdk5. We compared the extent of cell death in COS-7 cells transfected with p25/Cdk5 or p35/Cdk5 by purifying soluble fragmented DNA from these cells. DNA laddering, which was evident in p25/Cdk5-transfected cells, was present at a much reduced level in cells transfected with p35/Cdk5 or with empty vector (control cells) (Fig. 7i). We examined the nuclear morphology of infected cells by Hoechst stain. βgal-infected neurons had normal nuclear morphology (Fig. 7j, m), whereas most p25/Cdk5-infected neurons had fragmented and condensed nuclei (Figs 6l, 7k, n). Moreover, most of the p25/DNK5-infected neurons had normal nuclear morphology (Fig. 7l, o). Neurons with fragmented nuclei were also positive for the TdT-mediated dUTp nick end labelling (TUNEL) assay (data not shown). In general, more than 85% of p25/Cdk5-infected neurons had fragmented or condensed nuclear morphology, and the effect was largely reversed by the expression of DNK5 (Fig. 8a). Very few neurons had nuclear fragmentation after βgal viral infection. About 30% of p35/Cdk5-infected neurons had disrupted nuclei. These results were corroborated by calcium phosphate transfection of primary cortical neurons. A βgal DNA construct was cotransfected with various plasmid DNAs at a ratio of 1:5 to ensure that most positively scored βgal cells expressed the genes of interest. About 65–70% of p25/Cdk5-transfected neurons had fragmented nuclei, whereas less than 5% of neurons transfected with βgal alone and around 20% of those transfected with p35/Cdk5 had abnormal nuclear morphology (Fig. 8b). In addition, the p35 G2A mutant did not cause significant cell death (Fig. 8b). GSK3-β expression caused no detectable abnormalities in nuclear morphology in primary cortical neurons. The p25/Cdk5-induced nuclear condensation/fragmentation could be partially inhibited by Ac-DEVD-CHO, an inhibitor of caspase-3 (Fig. 8c).

The apoptotic cell bodies revealed by tubulin staining, DNA

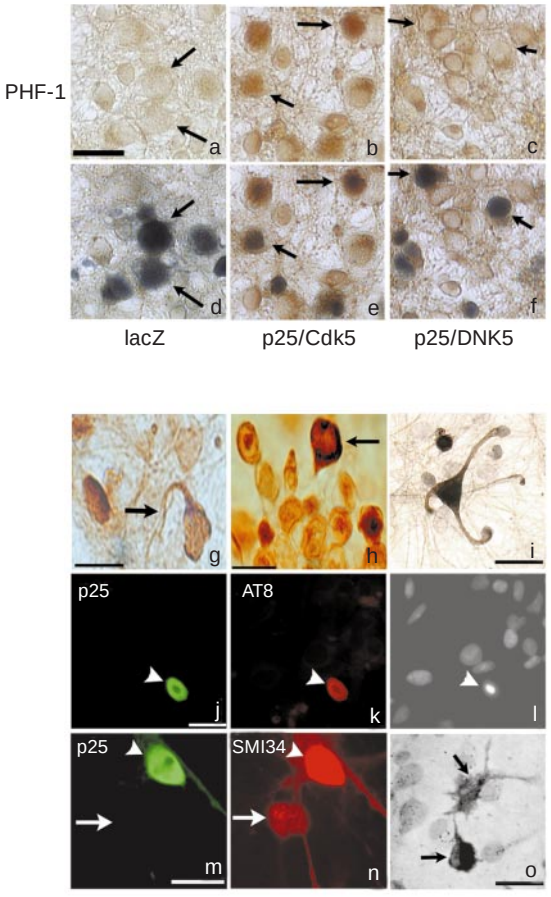

Figure 6 Effects of the p25/Cdk5 kinase on the neuronal cytoskeleton. Primary cortical cultures infected with βgal (**a, d**), p35 and Cdk5 (**g**), p25 and Cdk5 (**b, e, h, i, m–o**) and p25 and DNK5 (**c, f**) recombinant HSV viruses. Immunostaining for phospho-tau with PHF-1 (brown, **a**–**c** and **g**–**i**). **d**–**f**, Double labelling for either βgal (**d**) or p25 (**e**, **f**) to reveal infection-positive cells (dark blue). Arrows indicate positively infected neurons. **g**–**i**, High magnification of neurons infected with p35/Cdk5 (**g**, arrow labels neurite) and p25/Cdk5 (**h**, arrow labels neuron with enriched tau immunoreactive material in cell soma). **i**, p25/Cdk5-infected neuron with degenerated neurites, double labelled with PHF-1 (brown) and p25 antibodies (blue). **j–l**, Increased AT8 immunoreactivity in p25/Cdk5-transfected neurons. **j**, βgal-positive neuron (arrowhead) indicating transfected neuron. **k**, AT8 labelling of positively transfected neuron (arrowhead). **l**, Hoechst dye labelled nuclei depicting condensed nuclei (arrowhead) in p25/Cdk5-transfected neurons as compared to nontransfected cells. **m**, **n**, Phospho-neurofilament H (SMI34) fluorescent staining in **n** and p25 staining in **m** of p25/Cdk5-infected (arrowheads) and uninfected (arrows) neurons. **o**, Silver stain of p25/Cdk5-infected cultures (arrows) . All scale bars are 10 μm.

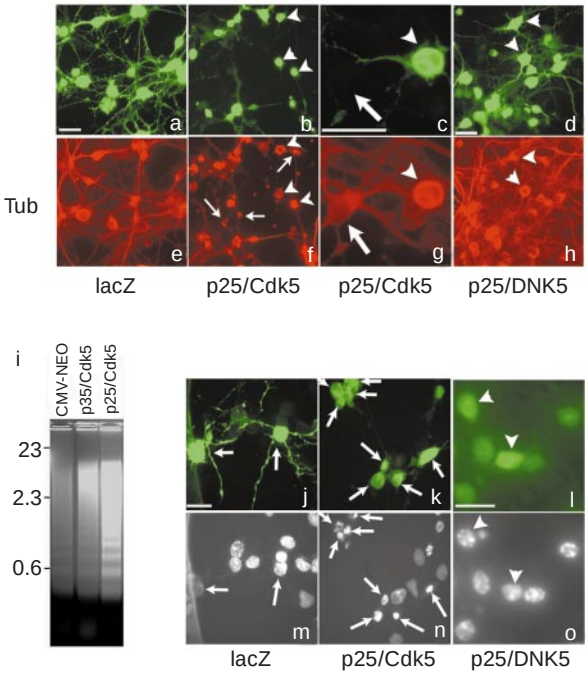

Figure 7 The p25/Cdk5 kinase induces cytoskeletal collapse and nuclear fragmentation. **a–h**, Cytoskeletal collapse; **j–o**, nuclear fragmentation. Fluorescent staining of neurons infected with βgal, p25/Cdk5 and p25/DNK5; βgal (green, **a** and **j**) and p25 (green, **b–d** and **k**, **l**), β-tubulin (red, **e–h**), or with Hoechst dye (**m–o**). In **b**, **c**, **2f** and **g** arrowheads indicate neurons devoid of most neurites; arrowheads in **d** and **h** indicate p25/DNK5-infected neurons; arrows in **f** indicate tubulin fragments (similar to apoptotic bodies); arrows in **c** and **g** indicate non-infected neurons. Arrows in **k** and **n** indicate infected neurons with apoptotic nuclear morphology; arrows in **j** and **m**, and arrowheads in **l** and **o**, indicate βgal- or p25/DNK5-infected neurons with normal nuclei. Scale bars are 10 μm. **i**, Soluble fragmented DNA purified from mock-, p35/Cdk5- and p25/Cdk5-transfected COS-7 cells.

laddering and fragmented and condensed nuclear morphology strongly support a pro-apoptotic effect for the p25/Cdk5 kinase. The inability of the catalytically inactive Cdk5 mutant to induce apoptosis indicates that substrate phosphorylation may be necessary for cell death. The reduction in apoptotic cell death resulting from p35/Cdk5 overexpression supports the idea that deregulation of Cdk5 is detrimental to cells. It further indicates that, in addition to the increase in kinase level, p25-mediated mislocalization of Cdk5 activity also contributes to the observed degeneration in neurons.

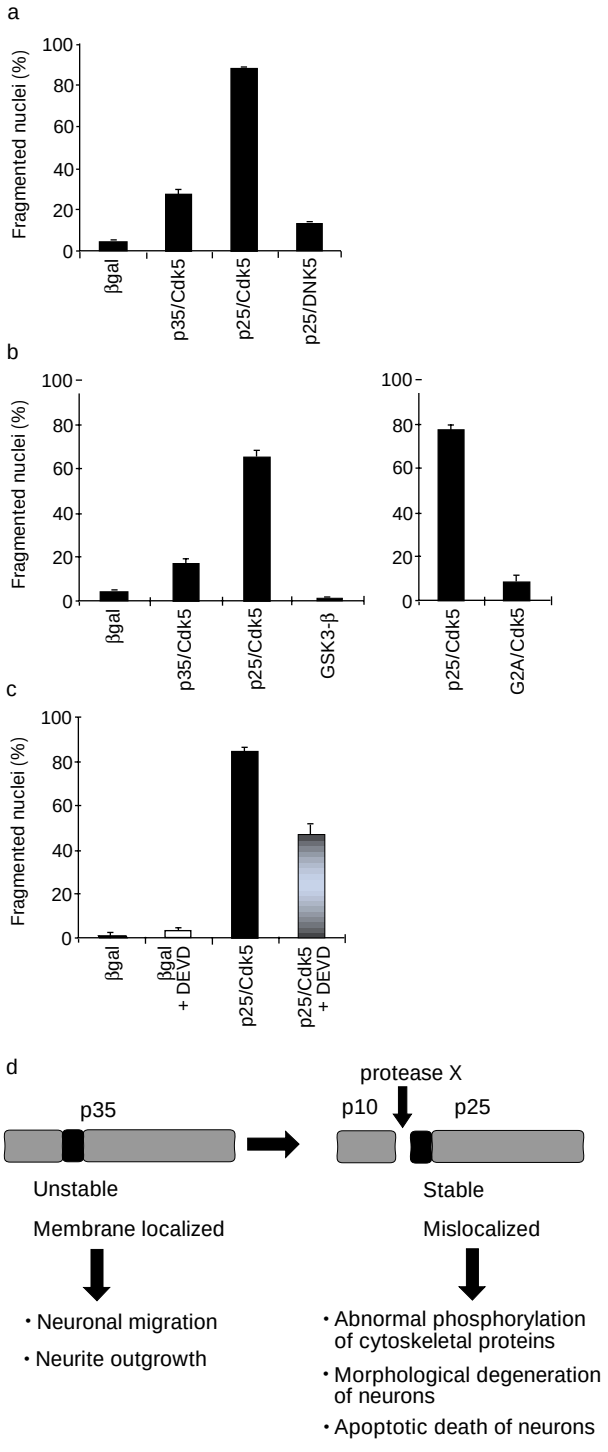

Figure 8 Quantification of nuclear fragmentation induced by the p25/Cdk5 kinase. **a–c**, Per cent fragmented nuclei of HSV-infected (**a**), calcium phosphate-transfected (**b**) and HSV-infected plus treated with DEVD inhibitor (**c**) cortical cultures. **d**, Model: cleavage of p35 and accumulation of p25 in neurons causes neuronal degeneration.

Discussion

We have shown that a proteolytic fragment of p35, p25, accumulates in the brains of AD patients and is present in neurons with NFT. Whereas p35 is required for normal brain development, the presence of p25 causes deregulation of Cdk5 kinase activity, due in part to the fact that p25 is a stable protein and that it is inappropriately localized. Other evidence indicates that the N-terminal portion of p35 may be necessary for binding to regulatory proteins[34]. Therefore, it is conceivable that, in neurons containing high levels of p25, Cdk5 is sequestered from normal regulation and concentrated at an abnormal site(s), and phosphorylates substrates not normally phosphorylated (or hyperphosphorylated) by this kinase. For instance, we show here that the p25/Cdk5 kinase displays an increased and altered tau phosphorylation in comparison to the p35/Cdk5 kinase *in vivo*. Neurofilament H is also heavily phosphorylated in p25/Cdk5-expressing neurons. Many reports indicate that hyperphosphorylation of microtubule-associated proteins such as tau alters their interactions with microtubules and causes microtubule instability. Indeed, tau phosphorylated by the p25/Cdk5 kinase displays reduced binding to microtubules. In addition, p25/Cdk5-expressing neurons showed neurite retraction and signs of microtubule collapse. Many of them could be labelled with a silver-based staining method which is commonly used as an indicator of cytoskeletal disruption. Thus, deregulation of Cdk5 by the accumulation of p25 impairs the integrity of the cytoskeleton, which ultimately results in morphological degeneration and, perhaps, neuronal apoptosis. Morphological degeneration and neuronal death are fundamental aspects of many neurodegenerative diseases. Our findings are nicely corroborated by the finding that the p35/Cdk5 kinase is associated with neuronal death[35–38]. Other possible deleterious effects of p25 are that it may prevent the p35/Cdk5 kinase from phosphorylating its normal substrates, such as Pak1, synapsin, syntaxin, Munc18 and DARP32 (refs 13, 20, 39 and 40) by sequestering Cdk5 from the cell periphery and nerve terminals, which also contributes to neuronal dysfunction.

We propose that conversion of p35 to p25 results in deregulation of the Cdk5 kinase. The deregulated Cdk5 kinase can cause irreversible damage to the cytoskeleton and neuronal death (Fig. 8d). On the basis of the accumulation of p25 in the brains of patients with AD and the cytoskeletal disruption and apoptosis induced by the p25/Cdk5 kinase in neurons, we suggest that p25 production and accumulation in the brain may contribute to the pathogenesis of AD. p25 may contribute to the early stages of AD, as it was not found to be accumulated in a terminal stage AD patient with significant cell loss. Futhermore, neurons with elevated p25 outnumbered neurons containing NFT in sections from the brains of AD patients. Thus, p25 accumulation may precede the formation of NFT. Conversion of p35 to p25 is likely to be the consequence of proteolytic cleavage; our preliminary results indicate that cleavage of p35 to p25 can be activated upon oxidative stress (Y. T. Kwon, M. S. Lee and L-H.T., unpublished data). It will be of interest to identify the putative protease that cleaves p35, as it may serve as a therapeutic target for prevention and treatment of neurodegenerative diseases.

Methods

Chemicals and antibodies

Cycloheximide (20 mg ml^{-1} stock; Sigma) was used at a final concentration of 30 μg ml^{-1} in $t_{1/2}$ experiments. Hoechst dye was also purchased from Sigma. The following antibodies were used: p35: polyclonal antibodies (pAb) neu-cyc (purified with either glutathione *S*-transferase (GST)–p10 (N-terminal—GST–p10 purified) or GST–p25 (C-terminal—GST–p25 purified)), 4E3 raised against whole protein[6], N-20 and C19 (Santa Cruz); Cdk5: monoclonal antibodies (mAb) DC17 (ref. 41), pAb C8 (Santa Cruz); haemagglutinin (HA): mAb 12CA5; mAb his_6 (Boehringer Mannheim); pAb βgal antibodies (Promega); pAb actin; mAb α- and β-tubulin (Sigma); tau: dephosphorylated tau epitopes at Ser 199

and Ser 202—mAb Tau-1 (Boehringer Mannheim)[42]; phosphorylated epitopes at Ser 396 and Ser 404—mAb PHF-1 (a gift from P. Davies)[43]; phosphorylated epitopes at N-terminal residues 2–10—mAb Alz-50 (a gift from P. Davies)[44]; AT8 (Innogenetics). The caspase-3 inhibitor Ac-DEVD-CHO was purchased from Sigma.

Constructs and viruses

Construction of CMV expression vectors for p10, p35, Cdk5 and DNK5 was as described[5]. CMV–p25 (amino acids 98–307) was made by polymerase chain reaction (PCR) using a 3′ p35 primer and 5′ deletion primer. CMV–p10 (amino acids 1–97) was made by PCR using a 5′ p35 primer and a 3′ deletion primer. The p10 fragment was then cloned upstream of a haemagglutinin (HA) tag. p35 Gly2Ala was made by site-directed mutagenesis[29] using the following oligo: 5′-CAGACACCATGGCCACGGTG-3′. Mutagenesis was verified by sequencing. Recombinant herpes simplex virus constructs (a gift from R. Neve) were made as described[45]. The following viruses were used: HSV–βgal, HSV–p35, HSV–p25, HSV–GFP–Cdk5 and HSV–GFP–DNK5 (where GFP is green fluorescent protein). Multiplicity of infection ranged from 0.1 to 1 for all viruses used. The HA–GSK3-β mammalian expression construct was a gift from X. He; the his_6–htau40 mammalian expression construct was a gift from D. Auprin (Pfizer)

Tissues and cell culture

We used brain tissue from eight patients with AD, four age-matched non-neurological cases and one patient with Huntington's disease. Brain lysates were made from Brodmann areas 11, 21 or 45 by Dounce homogenizing tissue in lysis buffer (50 mM Tris pH 7.5, 150 mM NaCl, 1% Triton-X, 10% glycerol, 5 mM EDTA, 1 mM EGTA, 1 mM DTT) plus inhibitors (2 μg ml^{-1} aprotinin, 2 μg ml^{-1} leupeptin, 1 μg ml^{-1} pepstatin, 50 mM β-glycerophosphate, 5 mM NaF, 5 mM $NaVO_3$ and 100 μg ml^{-1} PMSF). Lysates were cleared by centrifugation at 13,000*g* for 30 min. E17–19 pregnant rats (Long Evans strain) were purchased from Harland Sprague-Dawley. P0 pups were killed and their cortices were dissected and cultured as described[6]. Cortical cultures were grown in 24-well plates on either plastic or glass coverslips (400,000 cells per well) that had been treated with laminin and poly-D-lysine. Cultures were maintained in basal growth medium (BGM) for three days before viral infection. Swiss 3T3 and COS-7 cells were maintained in DMEM supplemented with 10% fetal calf serum. Ac-DEVD-CHO was added to medium (10 μM) ~8 h before infection and then every day (10 μM) after infection until cells were collected.

Transfection of COS-7 cells, cycloheximide treatment and kinase assays

COS-7 cells were transiently transfected with various plasmid constructs using calcium phosphate transfection procedures. For Fig. 3a, amounts of CMV plasmid DNA used were as follows: his_6–htau40 (5 μg), p35 (5 μg), p25 (2.5 μg), Cdk5 (5 μg), DNK5 (5 μg) and HA–GSK3-β (10 μg); for Fig. 3b we used five times as much p35 as p25 plasmid DNA. Cycloheximide $t_{1/2}$ experiments were performed as described[22]. Histone H1 kinase activity was determined as follows: ~1 mg of protein from brain lysates or transfected cell lysates was immunoprecipitated with p35 (4E3) or Cdk5 (C8) antibodies, respectively. Histone H1 was added as a substrate in the *in vitro* kinase assay performed as described[41]. In the case of p25 phosphorylation by Cdk5, no histone H1 was added. Subcellular fractionation was done as described[6,20].

Immunohistochemistry

P0 cortical cultures were infected with various combinations of HSV–βgal, HSV–p35, HSV–p25, HSV–GFP–Cdk5 and HSV–GFP–DNK5 after three days in culture. Two to three days after infection, cultures were fixed with acetone:methanol (1:1) for 3 min at room temperature (RT), washed three times with PBS and permeabilized with 0.2% Triton X-100 in blocking solution (1% blocking reagent (Boehringer Mannheim) in PBS) for 30 min at RT. Cultures were washed three times with PBS and incubated with either PHF-1 (1:100), AT8 (1:100), p35 (1:400) or βgal (1:400) antibodies for 12 h in blocking solution. The cultures were then washed three times with PBS, and rabbit or mouse secondary biotinylated antibodies were added (1:150) in blocking solution and detected by the Vector Elite substrate kit (Vector). Diaminobenzidine (DAB—brown) and Vector SG substrate (blue) were used in double-labelling experiments. Double labelling was performed sequentially.

Calcium phosphate transfection of cortical cultures (E17–19; after two days in culture) was performed as described[6]. A CMV–βgal plasmid (10 μg) was transfected with a CMV–NEO control plasmid (50 μg), CMV–p35 and CMV–Cdk5 (25 μg each), CMV–p25 and CMV–Cdk5 (25 μg each) or CMV–HA–GSK3-β (50 μg). Two to three days after transfection the cells were fixed and stained with βgal antibodies and Hoechst dye.

Transfected Swiss 3T3 cells were fixed with 4% paraformaldehyde and permeabilized in 0.3% Triton X-100. Immunostaining was done as described[6] using anti-HA (mAb 12CA5), anti-p25 (pAb neu-cyc, pAb N-20; Santa Cruz) and anti-actin (mAb; Sigma), to detect p35, p25, p35 G2A, HA-p10 and actin. The cells were then treated with biotin-conjugated anti-rabbit (followed by FITC-conjugated streptavidin) and Texas-Red-conjugated anti-mouse antibodies. Coverslips were mounted in ProLong antifade (Molecular Probes) and analysed using a Leica or Zeiss confocal microscope. Where stated, normal fluorescence microscopy was used.

For staining of control and AD brain tissue, paraffin sections (8 μm thick) were de-waxed in xylene, hydrated through graded alcohol solutions and blocked with 3% BSA, 10% NGS and 0.1% Triton X-100. The sections were incubated in citrate buffer for 10 min at 95 °C for antigen retrieval. The sections were incubated for 1 h at RT or overnight at 4 °C with 1–4 μg ml^{-1} of primary antibody. Bound rabbit and mouse antibodies were detected using Vectastain Elite Avidin-Biotin kit (Vector, Burlingame, CA) with DAB or Vector SG as substrate. For double-labelling studies, binding of the first primary antibody was detected as described, and binding of the second primary antibody was detected using DAB or Vector SG as substrate. At the conclusion of the immunostaining reactions, the sections were dehydrated and mounted with Permount (Fisher Scientific) under cover-glass.

A modified silver stain was used as described[46]. Infected cultures were fixed with 90% ethanol, 5% formaldehyde and 5% acetic acid before silver staining.

Microtubule-binding assay

The binding of tau to Taxol-stabilized microtubules (microtubules were assembled from purified bovine tubulin (Cytoskeleton) and stabilized by Taxol) was assayed as described[47]. Briefly, ~1 mg of 200,000*g* cell lysates (lysed in 100 mM PIPES, pH 6.8, 0.1% Triton X-100, 1 mM $MgCl_2$, 1 mM EGTA, 1 mM GTP plus inhibitors) from transfected cells were incubated with 100 μg Taxol-polymerized microtubules at 35 °C for 30 min. The microtubule-bound proteins were separated by centrifugation at 70,000*g* for 30 min. Pellets were resuspended in the same volume as supernatants and both bound and unbound fractions were analysed by western blot analysis.

Western blot analysis

P0 cortical cultures, brain lysates and transfected cells were washed with PBS and lysed with RIPA buffer plus inhibitors (2 μg ml^{-1} aprotinin, 2 μg ml^{-1} leupeptin, 1 μg ml^{-1} pepstatin, 5 mM NaF, 5 mM $NaVO_3$ and 100 μg ml^{-1} PMSF). In some cases, samples were immunoprecipitated with either p35 (polyclonal) or Cdk5 (C8) antibodies. Sample buffer was added to lysates and immunoprecipitates and samples were run on SDS–PAGE gels (see text and Figure 1egends for gel percentage), electrotransferred to nylon membrane and probed with either Tau-1 (1:2,000), PHF-1 (1:1,000), AT-8 (1:1,000), β-tubulin (1:2,000), anti-His_6 (1:2,000), anti-HA (12CA5; 1:25), DC17 (1:20) or p35 (C19; Santa Cruz) (1:2,000), p35 GST–p25 purified polyclonal (1:2,000) and GST–p10 purified polyclonal (1:1,000).

Cell death measurements and DNA laddering

After immunostaining, neurons or COS-7 cells were labelled with DNA dye Hoechst 33258 (2.5 μg ml^{-1}, 5 min), and infected neurons or transfected COS-7 cells were scored for healthy or apoptotic nuclear morphology. Cells were scored positive if they had a pyknotic and/or fragmented nucleus. Representative graphs are shown for experiments where 150 or 300 cells were scored. All experiments were done at least three times. TUNEL assays were done according to standard procedure (Boehringer Mannheim). For DNA laddering cells were lysed and soluble fragmented DNA was purified as described[48,49]. DNA was run on a 1.5% agarose gel.

Received 26 August; accepted 12 October 1999.

1. Lew, J., Winkfein, R. J., Paudel, H. K. & Wang, J. H. Brain proline-directed protein kinase is a neurofilament kinase which displays high sequence homology to p34cdc2. *J. Biol. Chem.* **267,** 25922–25926 (1992).
2. Meyerson, M. *et al.* A family of human cdc2-related protein kinases. *EMBO J.* **11,** 2909–2917 (1992).
3. Lew, J. *et al.* A brain-specific activator of cyclin-dependent kinase 5. *Nature* **371,** 423–426 (1994).
4. Ishiguro, K. *et al.* Identification of the 23 kDa subunit of tau protein kinase II as a putative activator of Cdk5 in bovine brain. *FEBS Lett.* **342,** 203–208 (1994).
5. Tsai, L. H., Delalle, I., Caviness, V. S. Jr, Chae, T. & Harlow, E. p35 is a neural-specific regulatory subunit of cyclin-dependent kinase 5. *Nature* **371,** 419–423 (1994).
6. Nikolic, M., Dudek, H., Kwon, Y. T., Ramos, Y. F. & Tsai, L. H. The Cdk5/p35 kinase is essential for neurite outgrowth during neuronal differentiation. *Genes Dev.* **10,** 816–825 (1996).
7. Paglini, G. *et al.* Evidence for the participation of the neuron-specific CDK5 activator P35 during laminin-enhanced axonal growth. *J. Neurosci.* **18,** 9858–9869 (1998).
8. Kwon, Y. T., Tsai, L. H. & Crandall, J. E. Callosal axon guidance defects in p35–/– mice. *J. Comp. Neurol* **415,** 218–229 (1999).
9. Kwon, Y. T. & Tsai, L. H. A novel disruption of cortical development in p35(–/–) mice distinct from reeler. *J. Comp. Neurol.* **395,** 510–522 (1998).
10. Chae, T. *et al.* Mice lacking p35, a neuronal specific activator of Cdk5, display cortical lamination defects, seizures, and adult lethality. *Neuron* **18,** 29–42 (1997).
11. Ohshima, T. *et al.* Targeted disruption of the cyclin-dependent kinase 5 gene results in abnormal corticogenesis, neuronal pathology and perinatal death. *Proc. Natl Acad. Sci. USA* **93,** 11173–11178 (1996).
12. Gilmore, E. C., Ohshima, T., Goffinet, A. M., Kulkarni, A. B. & Herrup, K. Cyclin-dependent kinase 5-deficient mice demonstrate novel developmental arrest in cerebral cortex. *J. Neurosci.* **18,** 6370–6377 (1998).
13. Bibb, J. A. *et al.* Phosphorylation of DARPP-32 by Cdk5 modulates dopamine signalling in neurons. *Nature* **402,** 669–671 (1999).
14. Fletcher, A. I. *et al.* Regulation of exocytosis by cyclin-dependent kinase 5 via phosphorylation of Munc18. *J. Biol. Chem.* **274,** 4027–4035 (1999).
15. Mandelkow, E. M. & Mandelkow, E. Tau in Alzheimer's disease. *Trends Cell Biol.* **8,** 425–427 (1998).
16. Spillantini, M. G. & Goedert, M. Tau protein pathology in neurodegenerative diseases. *Trends Neurosci.* **21,** 428–433 (1998).
17. Uchida, T. *et al.* Precursor of Cdk5 activator, the 23 kDa subunit of tau protein kinase II: its sequence and developmental change in brain. *FEBS Lett.* **355,** 35–40 (1994).
18. Biernat, J. *et al.* The switch of tau protein to an Alzheimer-like state includes the phosphorylation of two serine-proline motifs upstream of the microtubule binding region. *EMBO J.* **11,** 1593–1597 (1992).
19. Poon, R. Y., Lew, J. & Hunter, T. Identification of functional domains in the neuronal Cdk5 activator protein. *J. Biol. Chem.* **272,** 5703–5708 (1997).
20. Nikolic, M., Chou, M. M., Lu, W., Mayer, B. J. & Tsai, L. H. The p35/Cdk5 kinase is a neuron-specific Rac effector that inhibits Pak1 activity. *Nature* **395,** 194–198 (1998).

21. Philpott, A., Porro, E. B., Kirschner, M. W. & Tsai, L. H. The role of cyclin-dependent kinase 5 and a novel regulatory subunit in regulating muscle differentiation and patterning. *Genes Dev.* **11,** 1409–1421 (1997).
22. Patrick, G. N., Zhou, P., Kwon, Y. T., Howley, P. M. & Tsai, L. H. p35, the neuronal-specific activator of cyclin-dependent kinase 5 (Cdk5) is degraded by the ubiquitin-proteasome pathway. *J. Biol. Chem.* **273,** 24057–24064 (1998).
23. Imahori, K. *et al.* Possible role of tau protein kinases in pathogenesis of Alzheimer's disease. *Neurobiol. Aging* **19,** S93–98 (1998).
24. Baumann, K., Mandelkow, E. M., Biernat, J., Piwnica-Worms, H. & Mandelkow, E. Abnormal Alzheimer-like phosphorylation of tau-protein by cyclin-dependent kinases Cdk2 and Cdk5. *FEBS Lett.* **336,** 417–424 (1993).
25. Michel, G. *et al.* Characterization of tau phosphorylation in glycogen synthase kinase-3β and cyclin dependent kinase-5 activator (p23) transfected cells. *Biochim. Biophys. Acta* **1380,** 177–182 (1998).
26. Paudel, H. K. Phosphorylation by neuronal cdc2-like protein kinase promotes dimerization of Tau protein *in vitro*. *J. Biol. Chem.* **272,** 28328–28334 (1997).
27. Paudel, H. K., Lew, J., Ali, Z. & Wang, J. H. Brain proline-directed protein kinase phosphorylates tau on sites that are abnormally phosphorylated in tau associated with Alzheimer's paired helical filaments. *J. Biol. Chem.* **268,** 23512–23518 (1993).
28. Lovestone, S. *et al.* Alzheimer's disease-like phosphorylation of the microtubule-associated protein tau by glycogen synthase kinase-3 in transfected mammalian cells. *Curr. Biol.* **4,** 1077–1086 (1994).
29. Lovestone, S. & Reynolds, C. H. The phosphorylation of tau: a critical stage in neurodevelopment and neurodegenerative processes. *Neuroscience* **78,** 309–324 (1997).
30. Pant Veeranna, A. C., Pant, H. C. & Amin, N. Phosphorylation of human high molecular weight neurofilament protein (hNF-H) by neuronal cyclin-dependent kinase 5 (Cdk5). *Brain Res.* **765,** 259–266 (1997).
31. Sun, D., Leung, C. L. & Liem, R. K. H. Phosphorylation of the high molecular weight neurofilament protein (NF-H) by Cdk5 and p35. *J. Biol. Chem.* **271,** 14245–14251 (1996).
32. Guidato, S., Tsai, L. H., Woodgett, J. & Miller, C. C. Differential cellular phosphorylation of neurofilament heavy side-arms by glycogen synthase kinase-3 and cyclin-dependent kinase-5. *J. Neurochem.* **66,** 1698–1706 (1996).
33. Mandelkow, E. M. *et al.* Tau domains, phosphorylation, and interactions with microtubules. *Neurobiol. Aging* **16,** 355–362; discussion 362–353 (1995).
34. Lee, K. Y., Rosales, J. L., Tang, D. & Wang, J. H. Interaction of cyclin-dependent kinase 5 (Cdk5) and neuronal Cdk5 activator in bovine brain. *J. Biol. Chem.* **271,** 1538–1543 (1996).
35. Ahuja, H. S., Zhu, Y. & Zakeri, Z. Association of cyclin-dependent kinase 5 and its activator p35 with apoptotic cell death. *Dev. Genet.* **21,** 258–267 (1997).
36. Henchcliffe, C. & Burke, R. E. Increased expression of cyclin-dependent kinase 5 in induced apoptotic neuron death in rat substantia nigra. *Neurosci. Lett.* **230,** 41–44 (1997).
37. Shirvan, A. *et al.* Expression of cell cycle-related genes during neuronal apoptosis: is there a distinct pattern. *Neurochem. Res.* **23,** 767–777 (1998).
38. Zhang, Q., Ahuja, H. S., Zakeri, Z. F. & Wolgemuth, D. J. Cyclin-dependent kinase 5 is associated with apoptotic cell death during development and tissue remodeling. *Dev. Biol.* **183,** 222–233 (1997).
39. Matsubara, M. *et al.* Site-specific phosphorylation of synapsin I by mitogen-activated protein kinase and Cdk5 and its effects on physiological functions. *J. Biol. Chem.* **271,** 21108–21113 (1996).
40. Shuang, R. *et al.* Regulation of Munc-18/syntaxin 1A interaction by cyclin-dependent kinase 5 in nerve endings. *J. Biol. Chem.* **273,** 4957–4966 (1998).
41. Tsai, L. H., Takahashi, T., Caviness, V. S. Jr & Harlow, E. Activity and expression pattern of cyclin-dependent kinase 5 in the embryonic mouse nervous system. *Development* **119,** 1029–1040 (1993).
42. Binder, L. I., Frankfurter, A. & Rebhun, L. I. The distribution of tau in the mammalian central nervous system. *J. Cell Biol.* **101,** 1371–1378 (1985).
43. Greenberg, S. G., Davies, P., Schein, J. D. & Binder, L. I. Hydrofluoric acid-treated tau PHF proteins display the same biochemical properties as normal tau. *J. Biol. Chem.* **267,** 564–569 (1992).
44. Wolozin, B. L., Pruchnicki, A., Dickson, D. W. & Davies, P. A neuronal antigen in the brains of Alzheimer patients. *Science* **232,** 648–650 (1986).
45. Bursztajn, S. *et al.* Overexpression in neurons of human presenilin-1 or a presenilin-1 familial Alzheimer disease mutant does not enhance apoptosis. *J. Neurosci.* **18,** 9790–9799 (1998).
46. Fix, A. S., Ross, J. F., Stitzel, S. R. & Switzer, R. C. Integrated evaluation of central nervous system lesions: stains for neurons, astrocytes, and microglia reveal the spatial and temporal features of MK-801-induced neuronal necrosis in the rat cerebral cortex. *Toxicol. Pathol.* **24,** 291–304 (1996).
47. Tanaka, T., Iqbal, K., Trenkner, E., Liu, D. J. & Grundke-Iqbal, I. Abnormally phosphorylated tau in SY5Y human neuroblastoma cells. *FEBS Lett.* **360,** 5–9 (1995).
48. Hockenbery, D., Nunez, G., Milliman, C., Schreiber, R. D. & Korsmeyer, S. J. Bcl-2 is an inner mitochondrial membrane protein that blocks programmed cell death. *Nature* **348,** 334–336 (1990).
49. Xia, Z., Dickens, M., Raingeaud, J., Davis, R. J. & Greenberg, M. E. Opposing effects of ERK and JNK-p38 MAP kinases on apoptosis. *Science* **270,** 1326–1331 (1995).

Acknowledgements

We thank D. Auprin, P. Davies, X. He, R. Neve and J. P. Vonsattel for reagents; Y. Zhou for antibody preparations; D. Smith for help with microscopy; and M. Greenberg, P. Lu, Y. Shi, G. Gill, Y. T. Kwon, D. Smith, V. Tannoch and J. Volker for critical reading of this manuscript. This work was partially supported by NIH grants to L.-H.T. L.-H.T. is an assistant investigator of the Howard Hughes Medical Institute, a Rita Allen Foundation scholar and a recipient of an Ester A. and Joseph Klingenstein Fund award.

Correspondence and requests for materials should be addressed to L.-H.T. (e-mail: li-huei_tsai@hms.harvard.edu).